Journal of Inorganic Biochemistry 104 (2010) 297–309

Contents lists available at ScienceDirect

Journal of Inorganic Biochemistry

journal homepage: www.elsevier.com/locate/jinorgbio

Water-soluble cationic gallium(III) and indium(III) phthalocyanines for photodynamic therapy

Mahmut Durmuş [a], Vefa Ahsen [a,b,*]

[a] *Gebze Institute of Technology, Department of Chemistry, PO Box 141, Gebze 41400, Kocaeli, Turkey*
[b] *TUBITAK-Marmara Research Centre, Materials Institute, PO Box 21, Gebze 41470, Kocaeli, Turkey*

ARTICLE INFO

Article history:
Received 31 May 2009
Received in revised form 8 December 2009
Accepted 16 December 2009
Available online 18 January 2010

Keywords:
Phthalocyanine
Water soluble
Gallium
Indium
Photodynamic therapy
Photosensitizer

ABSTRACT

The new tetra-non-peripheral and peripheral 2-mercaptopyridine substituted gallium(III) and indium(III) phthalocyanine complexes (**np-GaPc, p-GaPc, np-InPc** and **p-InPc**) and their quaternized derivatives (**Qnp-GaPc, Qp-GaPc, Qnp-InPc** and **Qp-InPc**) have been synthesized and characterized. The quaternized complexes show excellent solubility in water, which makes them potential photosensitizer for use in photodynamic therapy (PDT) of cancer. Photophysical and photochemical properties of these phthalocyanines were investigated. General trends are described for quantum yields of photodegradation, fluorescence and fluorescence lifetimes as well as singlet oxygen quantum yields of these compounds. In this study, the effects of the position of the substituents, the nature of the metal ion and quaternization of the substituents on the photophysical and photochemical parameters of the gallium(III) and indium(III) phthalocyanines are also reported. This study also presented the ionic gallium(III) and indium(III) phthalocyanines strongly bind to bovine serum albumin (BSA).

1. Introduction

Phthalocyanines (Pc) and metallophthalocyanines (MPc) have been studied in great deal for many years, mostly in terms of their uses as dyes and catalysts [1–3]. Recently, they have also found applications in many fields ranging from industrial [4], technological [5,6] to medical [7,8]. The Pc macrocycle can engage most metal ions in its cavity; hence scores of different MPc complexes have been synthesized. The nature of the metal ion coordinated within the Pc cavity plays a vital role in the properties, reactions and of course, applications of the resulting MPc. MPc derivatives in which the central metal is diamagnetic and non-transitional, are photoactive, and are often employed in photosensitization and energy conversion [9,10]. Worth emphasizing, is the Pcs' application as photosensitizers in the photodynamic therapy (PDT) of tumours. MPc complexes have been proved as highly promising photosensitizers for PDT due to their intense absorption in the red region of the visible light. High triplet state quantum yields and long triplet lifetimes are required for efficient sensitization of them. The photophysical properties of the Pc dyes are strongly influenced by the presence and nature of the central metal ion. Complex structure of Pc with transition metals gives short triplet lifetimes to these dyes. Closed shell and diamagnetic ions, such as Zn^{2+}, Ga^{3+} and Si^{4+}, give Pc complexes with both high triplet yields and long lifetimes [11–14].

The photophysics and photochemistry of gallium(III) and indium(III) Pc complexes are well documented [15–18]. Such studies reveal that these complexes show great promise for photocatalytic and photosensitizing applications [19,20]. However, studies on water-soluble gallium(III) and indium(III) Pc complexes are scarce in the literature [21,22].

In PDT administration, the drug is injected into the patient's blood stream, and since the blood itself is a hydrophilic system, water solubility becomes crucial for a potential photosensitizer in PDT. The advantages of MPcs bearing cationic substituents over those with neutral and anionic substituents are numerous [23], and include the following: (i) they are able to improve water solubility and prevent aggregation [24]; aggregation seriously compromises the PDT value of the photosensitizer, (ii) they are more efficient as PDT agents [25] and also improve cell uptake [26], (iii) they are selectively localized in the cell mitochondria, which when impaired induces apoptosis [27].

Thiol-derivatized MPc complexes show rich spectroscopic and photochemical properties. For example, they are known to absorb at longer wavelengths (>700 nm) [28,29] than other MPc complexes. Therefore these complexes have a very useful feature for applications in optoelectronics, near-IR devices and PDT.

The advantages that go with cation-substituted MPcs are too striking to overlook, hence our interest in these complexes. In this

---

[*] Corresponding author. Address: Gebze Institute of Technology, Department of Chemistry, PO Box 141, Gebze 41400, Kocaeli, Turkey. Tel.: +90 2626053106; fax: +90 2626053101.
E-mail address: ahsen@gyte.edu.tr (V. Ahsen).

doi:10.1016/j.jinorgbio.2009.12.011

work, the synthesis, photophysical and photochemical studies on new non-peripheral and peripheral tetra-substituted non-ionic and quaternized ionic gallium(III) and indium(III) Pc complexes (Schemes 1 and 2) are presented. The aim of our ongoing research is to synthesis water-soluble gallium(III) and indium(III) Pc complexes to be used as potential PDT agents, since gallium(III) and indium(III) Pc complexes show good photophysical and photochemical properties which are very useful for PDT studies. Herein, we report the synthesis, characterization and spectroscopic behaviour as well as photophysical (fluorescence quantum yields and lifetimes) and photochemical (singlet oxygen and photodegradation quantum yields) properties of gallium(III) and indium(III) Pc complexes tetra-substituted at the non-peripheral (**np-GaPc** and **np-InPc**) and peripheral (**p-GaPc** and **p-InPc**) positions with 2-mercaptopyridine group (Scheme 1) and their quaternized (**Qnp-GaPc** and **Qnp-InPc** for non-peripheral, **Qp-GaPc** and **Qp-InPc** for peripheral position) complexes (Scheme 2).

Bovine serum albumin (BSA) and human serum albumin (HSA) are major plasma proteins, which contribute significantly to physiological functions and display effective drug delivery roles [30,31], hence the investigation of binding of drugs with albumin is of interest. A spectroscopic investigation of the binding of the water-soluble gallium(III) and indium(III) Pc complexes (**Qnp-GaPc, Qp-GaPc, Qnp-InPc** and **Qp-InPc**) to BSA is also presented in this work.

2. Experimental

2.1. Materials

Quinoline, DMSO, methanol, *n*-hexane, ethylacetate, CCl_4, diethylether, chloroform ($CHCl_3$), dichloromethane (DCM), tetrahydrofuran (THF), acetone, ethanol and dimethylformamide (DMF) were dried as described in Perrin and Armarego [32] before use. Zinc phthalocyanine, anhydrous gallium(III) chloride, anhydrous indium(III) chloride, K_2CO_3, dimethylsulphate (DMS) were purchased from Aldrich. 2-Mercaptopyridine, 1,8-diazabicyclo[5.4.0]undec-7-ene (DBU), 9,10-antracenediyl-bis(methylene)dimalonoic acid (ADMA) and 1,3-diphenylisobenzofuran (DPBF) were purchased from Fluka. Preparative thin layer chromatography was performed on silica gel 60 P F_{254}. 3-Nitrophthalonitrile (**1**) [33], 4-nitrophthalonitrile (**2**) [34], 3-(2-mercaptopyridine) phthalonitrile (**3**) and 4-(2-mercaptopyridine) phthalonitrile (**4**) [35] were synthesized and purified according to literature procedures.

2.2. Equipment

Absorption spectra in the UV–visible region were recorded with a Shimadzu 2001 UV spectrophotometer. Fluorescence excitation and emission spectra were recorded on a Varian Eclipse spectrofluorometer using 1 cm pathlength cuvettes at room temperature. IR spectra (KBr pellets) were recorded on a Bio-Rad FTS 175C FTIR spectrometer. The mass spectra were acquired on a Bruker Daltonics (Bremen, Germany) MicrOTOF mass spectrometer equipped with electronspray ionization (ESI) source. The instrument was operated in positive ion mode using a *m/z* range of 50–3000. The capillary voltage of the ion source was set at 6000 V and the capillary exit at 190 V. The nebulizer gas flow was 1 bar and drying gas flow 8 mL/min. The drying temperature was set at 200 °C for quaternized complexes (**Qnp-GaPc, Qp-GaPc, Qnp-InPc** and **Qp-InPc**). ^1H NMR spectra were recorded in DMSO-d_6 solutions on a Varian 500 MHz spectrometer. Elemental analyses were obtained with a Thermo Finnigan Flash 1112 Instrument. Although the elemental analysis data for one or two atoms for several compounds are

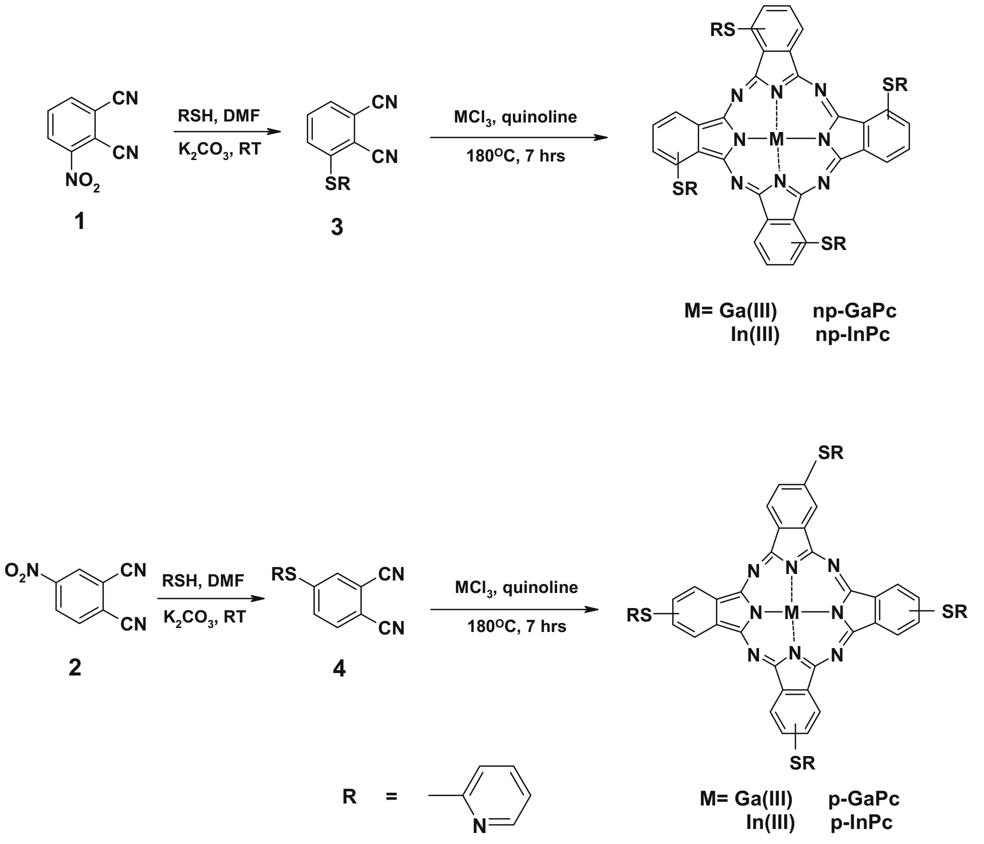

Scheme 1. Synthesis of tetra-2-mercaptopyridine substituted gallium(III) and indium(III) phthalocyanine complexes.

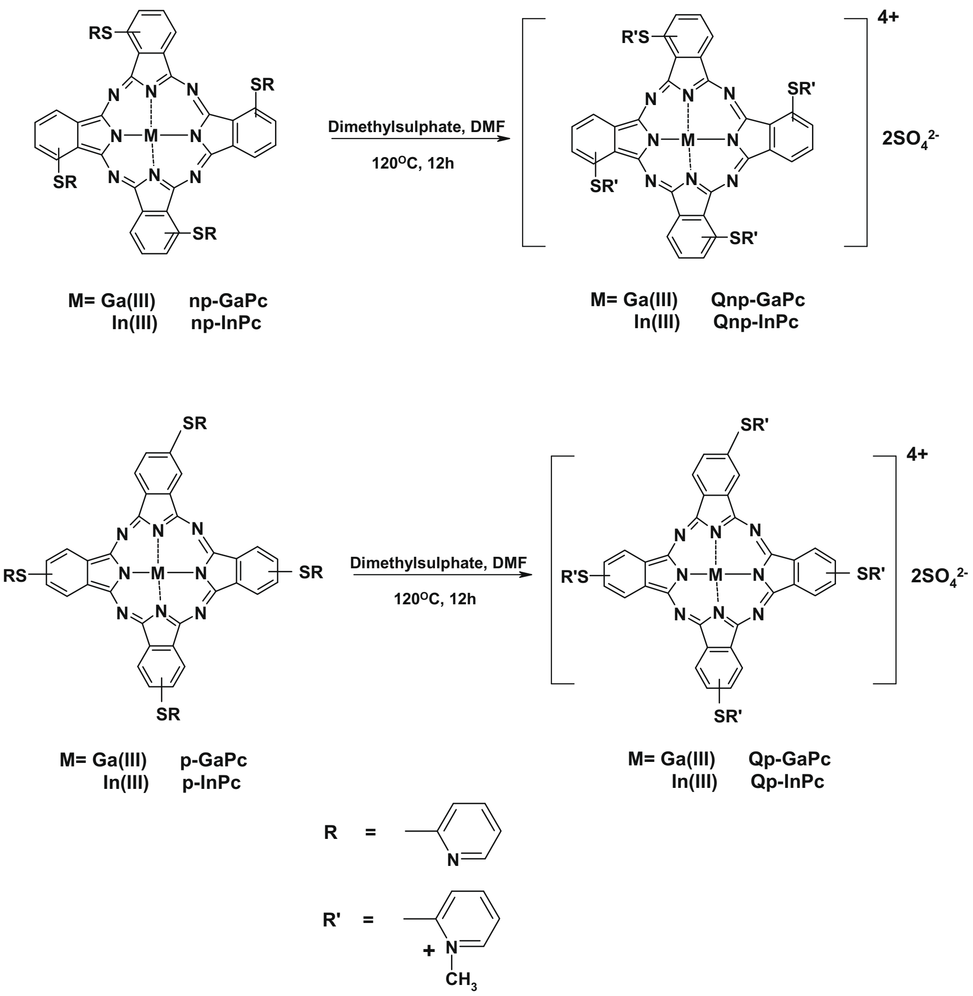

Scheme 2. Synthesis of tetra-2-mercaptopyridine substituted quaternized gallium(III) and indium(III) phthalocyanine complexes.

somewhat (>0.5%) unsatisfactory, the ESI-MS results and other spectroscopic analysis (^{1}H NMR, IR) data reasonably support the chemical formulas.

Photo-irradiations were done using a General Electric quartz line lamp (300 W). A 600 nm glass cut off filter (Schott) and a water filter were used to filter off ultraviolet and infrared radiations respectively. An interference filter (Intor, 670 or 700 nm with a band width of 40 nm) was additionally placed in the light path before the sample. Light intensities were measured with a POWER MAX5100 (Molelectron detector incorporated) power meter.

2.3. Photophysical parameters

2.3.1. Fluorescence quantum yields and lifetimes

Fluorescence quantum yields (Φ_F) were determined by the comparative method (Eq. (1)) [36,37],

$$\Phi_F = \Phi_F(\mathrm{Std}) \frac{F \cdot A_{\mathrm{Std}} \cdot \eta^2}{F_{\mathrm{Std}} \cdot A \cdot \eta^2_{\mathrm{Std}}} \quad (1)$$

where F and F_{Std} are the areas under the fluorescence emission curves of the samples (Schemes 1 and 2) and the standard, respectively. A and A_{Std} are the respective absorbances of the samples and standard at the excitation wavelengths, respectively. η^2 and η^2_{Std} are the refractive indices of solvents used for the sample and standard, respectively. Unsubstituted ZnPc (in DMSO) ($\Phi_F = 0.18$) [38] was employed as the standard. The absorbance of the solutions at the excitation wavelength ranged between 0.04 and 0.05.

Natural radiative life times (τ_0) were determined using PhotochemCAD program which uses the Strickler–Berg equation [39]. The fluorescence lifetimes (τ_F) were evaluated using Eq. (2).

$$\Phi_F = \frac{\tau_F}{\tau_0} \quad (2)$$

2.4. Photochemical parameters

2.4.1. Singlet oxygen quantum yields

Singlet oxygen quantum yield (Φ_Δ) determinations were carried out using the experimental set-up described in the literature [40,41]. Typically, a 3 mL portion of the respective unsubstituted, peripheral and non-peripheral tetra-substituted gallium(III) and indium(III) Pc solutions (absorbance ~1.0 at the irradiation wavelength) containing the singlet oxygen quencher was irradiated in the Q band region with the photo-irradiation set-up described in references [40,41]. Φ_Δ values were determined in air using the relative method with ZnPc (in DMSO) or ZnPcS$_{\mathrm{mix}}$ (in aqueous media) as references. DPBF and ADMA were used as chemical quenchers for singlet oxygen in DMSO and aqueous media, respectively. Eq. (3) was employed for the calculations:

$$\Phi_\Delta = \Phi_\Delta^{\mathrm{Std}} \frac{\mathrm{R} \cdot \mathrm{I}_{\mathrm{abs}}^{\mathrm{Std}}}{\mathrm{R}^{\mathrm{Std}} \cdot \mathrm{I}_{\mathrm{abs}}} \quad (3)$$

where Φ_Δ^{Std} is the singlet oxygen quantum yields for the standard ZnPc ($\Phi_\Delta^{Std} = 0.67$ in DMSO) [42] and ZnPcS$_{mix}$ ($\Phi_\Delta^{Std} = 0.45$ in aqueous media) [41], R and R_{Std} are the DPBF (or ADMA) photobleaching rates in the presence of the respective samples (Schemes 1 and 2) and standards, respectively. I_{abs} and I_{abs}^{Std} are the rates of light absorption by the samples and standards, respectively. To avoid chain reactions induced by DPBF (or ADMA) in the presence of singlet oxygen [43], the concentration of quenchers (DPBF or ADMA) was lowered to $\sim 3 \times 10^{-5}$ M. Solutions of sensitizer (absorbance = 1 at the irradiation wavelength) containing DPBF (or ADMA) were prepared in the dark and irradiated in the Q band region using the set-up described above. DPBF degradation at 417 nm and ADMA degradation at 380 nm were monitored. The light intensity 6.65×10^{15} photons s^{-1} cm^{-2} was used for Φ_Δ determinations.

2.4.2. Photodegradation quantum yields

Photodegradation quantum yield (Φ_d) determinations were carried out using the experimental set-up described in literature [40,41]. Photodegradation quantum yields were determined using Eq. (4):

$$\Phi_d = \frac{(C_0 - C_t) \cdot V \cdot N_A}{I_{abs} \cdot S \cdot t} \tag{4}$$

where C_0 and C_t are the samples concentrations before and after irradiation respectively, V is the reaction volume, N_A the Avogadro's constant, S the irradiated cell area and t the irradiation time, I_{abs} is the overlap integral of the radiation source light intensity and the absorption of the samples. A light intensity of 2.23×10^{16} photons s^{-1} cm^{-2} was employed for Φ_d determinations.

2.4.3. Binding of quaternized gallium(III) and indium(III) Pc complexes to BSA

The binding of the quaternized gallium(III) and indium(III) Pc complexes (**Qnp-GaPc, Qp-GaPc, Qnp-InPc** and **Qp-InPc**) to BSA were studied by spectrofluorometry at room temperature. An aqueous solution of BSA (fixed concentration) was titrated with varying concentrations of the respective quaternized gallium(III) and indium(III) Pc solutions. BSA was excited at 280 nm and fluorescence recorded between 290 nm and 500 nm. The steady diminution in BSA fluorescence with increase in quaternized gallium(III) and indium(III) Pc concentrations was noted and used in the determination of the binding constants and the number of binding sites on BSA, according to Eq. (5) [44–46].

$$\log\left[\frac{(F_0 - F)}{(F - F_\infty)}\right] = \log \mathrm{K}_b + n \log[\mathrm{Pc}] \tag{5}$$

where F_0 and F are the fluorescence intensities of BSA in the absence and presence of quaternized Pc complexes (**Qnp-GaPc, Qp-GaPc, Qnp-InPc** and **Qp-InPc**) respectively; F_∞, the fluorescence intensity of BSA saturated with quaternized Pc complexes; K_b, the binding constant; n, the number of binding sites on a BSA molecule; and [Pc] the concentration of quaternized Pc complexes. Plots of $\log\left[\frac{(F_0-F)}{(F-F_\infty)}\right]$ against log[Pc] would provide the values of n (from the slope) and K_b (from the intercept).

The changes in BSA fluorescence intensity were related to quaternized Pc concentrations by the Stern–Volmer relationship (Eq. (6)):

$$\frac{F_0^{BSA}}{F^{BSA}} = 1 + K_{SV}^{BSA}[\mathrm{Pc}] \tag{6}$$

and K_{SV}^{BSA} is given by Eq. (7):

$$K_{SV}^{BSA} = k_q \tau_{F(BSA)} \tag{7}$$

where F_0^{BSA} and F^{BSA} are the fluorescence intensities of BSA in the absence and presence of quaternized Pc complexes (**Qnp-GaPc, Qp-GaPc, Qnp-InPc** and **Qp-InPc**) respectively; K_{SV}^{BSA}, the Stern–Volmer quenching constant; k_q, the bimolecular quenching constant; and $\tau_{F(BSA)}$, the fluorescence lifetime of BSA. $\tau_{F(BSA)}$ is known to be 10 ns [47–49], thus from the values of K_{SV}^{BSA} obtained from the plots of F_0^{BSA}/F^{BSA} versus [Pc], the value of k_q may be determined (Eq. (7)).

2.5. Synthesis

2.5.1. 1,(4)-Tetrakis-[(2-mercaptopyridine)phthalocyaninato] chlorogallium(III) (***np-GaPc***, Scheme 1)

A mixture of anhydrous gallium(III) chloride (0.74 g, 4.22 mmol), 3-(2-mercaptopyridine) phthalonitrile (**3**) (1.00 g, 4.22 mmol), DBU (0.1 mL, 0.7 mmol) and quinoline (5 mL, doubly distilled over CaH$_2$) was stirred at 180 °C for 7 h under nitrogen atmosphere. After cooling, the solution was dropped in the *n*-hexane. The green solid product was precipitated and collected by filtration and washed with *n*-hexane. The crude product was dissolved in chloroform. After concentrating, the dark green waxy product was precipitated with hot *n*-hexane. Furthermore the crude green product was purified by column chromatography over Al$_2$O$_3$ using ethyl acetate/methanol (5:1) solvent system as an eluent. Green solid product was obtained. MP > 240 °C, Yield: 0.36 g (32%). UV/visible (UV/Vis) (DMSO): λ_{max} nm (log ε) 346 (4.53), 642 (4.22), 716 (4.88). IR [(KBr) ν_{max}/cm^{-1}]: 3045 (Ar-CH), 1595 (C=N), 1570 (C=C), 1449, 1418, 1317, 1107, 908, 762, 744. ^{1}H NMR (DMSO-d$_6$, *m* = multiplet): δ, ppm 9.62–9.57 (m, 4H, Pyridyl-H), 8.66–8.59 (m, 4H, Pyridyl-H), 8.34–8.09 (m, 8H, Pyridyl-H and Pc-H), 7.86–7.78 (m, 8H, Pyridyl-H and Pc-H), 7.39–7.33 (m, 4H, Pc-H). Calc. for C$_{52}$H$_{28}$N$_{12}$S$_4$GaCl: C 59.24, H 2.68, N 15.94%; Found: C 58.91, H 2.44 N 16.09%. MS (ESI-MS) *m/z*: Calc. 1054.1; Found: 1055.0 [M+1]$^+$, 1019.2 [M−Cl]$^+$.

2.5.2. 1,(4)-Tetrakis-[(2-mercaptopyridine)phthalocyaninato] chloroindium(III) (***np-InPc***, Scheme 1)

Synthesis and purification was as outlined for ***np-GaPc*** except anhydrous indium(III) chloride was employed instead of anhydrous gallium(III) chloride. The amounts of the reagents employed were: **3** (1.00 g, 4.22 mmol), DBU (0.1 mL, 0.7 mmol), anhydrous indium(III) chloride (0.93 g , 4.22 mmol) in quinoline (5 mL). The crude green product was purified by column chromatography over silica gel using ethyl acetate and then CH$_2$Cl$_2$/methanol (10:1) solvent system as an eluent. MP > 240 °C, Yield: 0.45 g (39%). UV/Vis (DMSO): λ_{max} nm (log ε) 345 (4.62), 642 (4.31), 714 (4.99). IR [(KBr) ν_{max}/cm^{-1}]: 3049 (Ar-CH), 1627 (C=N), 1575 (C=C), 1449, 1417, 1327, 1102, 898, 757, 742. ^{1}H NMR (DMSO-d$_6$): δ, ppm 9.10–8.92 (m, 4H, Pyridyl-H), 8.69–8.51 (m, 4H, Pyridyl-H), 8.11–7.93 (m, 8H, Pyridyl-H and Pc-H), 7.79–7.58 (m, 8H, Pyridyl-H and Pc-H), 7.30–7.24 (m, 4H, Pc-H). Calc. for C$_{52}$H$_{28}$N$_{12}$S$_4$InCl: C 56.81, H 2.57, N 15.29%; Found: C 56.41, H 2.19 N 15.83%. MS (ESI-MS) *m/z*: Calc. 1098.2; Found: 1099.0 [M+1]$^+$.

2.5.3. 2,(3)-Tetrakis-[(2-mercaptopyridine)phthalocyaninato] chlorogallium(III) (***p-GaPc***, Scheme 1)

Synthesis and purification was as outlined for ***np-GaPc*** except 4-(2-mercaptopyridine) phthalonitrile (**4**) was employed instead of 3-(2-mercaptopyridine) phthalonitrile (**3**). The amounts of the reagents employed were: **4** (1.00 g, 4.22 mmol), DBU (0.1 mL, 0.7 mmol), anhydrous gallium(III) chloride (0.74 g, 4.22 mmol) in quinoline (5 mL). The crude green product was purified by column chromatography over silica gel using ethyl acetate and then CH$_2$Cl$_2$/methanol (10:1) solvent system as an eluent. MP > 240 °C, Yield: 0.45 g (41%). UV/Vis (DMSO): λ_{max} nm (log ε) 362 (4.63), 622 (4.39), 695 (5.16). IR [(KBr) ν_{max}/cm^{-1}]: 3049 (Ar-CH), 1645 (C=N), 1573 (C=C), 1448, 1417, 1309, 1118, 919, 764, 747. ^{1}H NMR (DMSO-d$_6$, br = broad): δ, ppm 9.73–9.58 (m, 8H, Pyridyl-H), 8.57–8.49 (m, 8H, Pyridyl-H and Pc-H), 7.80 (br, 4H, Pyridyl-H),

Table 1
Absorption, excitation and emission spectral data for unsubstituted, non-peripheral and peripheral tetra-substituted gallium(III) and indium(III) phthalocyanine complexes in DMSO and water.

Compound	Solvent	Q band λ_{max}, (nm)	(log ε)	Excitation λ_{Ex}, (nm)	Emission λ_{Em}, (nm)	Stokes shift Δ_{Stokes}, (nm)
GaPc[a]	DMSO	680	5.15	680	691	11
np-GaPc	DMSO	716	4.88	717	737	21
p-GaPc	DMSO	695	5.16	694	708	13
Qnp-GaPc	DMSO	701	5.02	699	708	7
	H_2O	686, 653	4.52, 4.53	689	702	16
Qp-GaPc	DMSO	689	4.94	689	702	13
	H_2O	685	4.83	686	697	12
InPc[a]	DMSO	686	4.46	689	700	14
np-InPc	DMSO	714	4.99	727	732	18
p-InPc	DMSO	695	5.17	697	712	17
Qnp-InPc	DMSO	703	4.95	696	711	8
	H_2O	685, 652	4.59, 4.57	–	–	–
Qp-InPc	DMSO	692	4.80	700	711	19
	H_2O	686, 649	4.40, 4.46	700	701	15

[a] Data from [55].

7.49–7.45 (m, 4H, Pc-H), 7.30 (br, 4H, Pc-H). Calc. for $C_{52}H_{28}N_{12}S_4GaCl$: C 59.24, H 2.68, N 15.94%; Found: C 58.67, H 2.79 N 16.22%. MS (ESI-MS) *m*/*z*: Calc. 1054.1; Found: 1055.0 $[M+1]^+$, 1019.2 $[M-Cl]^+$.

2.5.4. 2,(3)-Tetrakis-[(2-mercaptopyridine)phthalocyaninato] chloroindium(III) (***p-InPc***, Scheme 1)

Synthesis and purification was as outlined for ***np-GaPc*** except 4-(2-mercaptopyridine) phthalonitrile (**4**) was employed instead of 3-(2-mercaptopyridine) phthalonitrile (**3**) and anhydrous indium(III) chloride was employed instead of anhydrous gallium(III) chloride. The amounts of the reagents employed were: **4** (1.00 g, 4.22 mmol), DBU (0.1 mL, 0.7 mmol), anhydrous indium(III) chloride (0.93 g, 4.22 mmol) in quinoline (5 mL). The crude green product was purified by column chromatography over silica gel using ethyl acetate and then CH_2Cl_2/methanol (10:1) solvent system as an eluent. MP > 240 °C, Yield: 0.53 g (46%). UV/Vis (DMSO): λ_{max} nm (log ε) 372 (4.72), 623 (4.44), 695 (5.17). IR [(KBr) ν_{max}/cm^{-1}]: 3054 (Ar-CH), 1601 (C=N), 1573 (C=C), 1448, 1417, 1338, 1118, 911, 760, 742. ^1H NMR (DMSO-d_6): δ, ppm 9.37–9.08 (m, 8H, Pyridyl-H), 8.84–8.81 (m, 4H, Pc-H), 8.57–8.51 (m, 4H, Pyridyl-H), 8.03 (br, 4H, Pyridyl-H), 7.75 (br, 4H, Pc-H), 7.52 (br, 4H, Pc-H). Calc. for $C_{52}H_{28}N_{12}S_4InCl$: C 56.81, H 2.57, N 15.29%; Found: C 56.35, H 2.20 N 15.90%. MS (ESI-MS) *m*/*z*: Calc. 1098.2; Found: 1099.0 $[M+1]^+$.

2.5.5. 1,(4)-Tetrakis-[(N-methyl-2-mercaptopyridine)phthalocyaninato] chlorogallium(III) sulphate (***Qnp-GaPc***, Scheme 2)

Compound ***np-GaPc*** (190 mg, 0.177 mmol) was heated to 120 °C in freshly distilled DMF (5 mL) and excess DMS (0.168 mL, 1.77 mmol) was added dropwise. The mixture was stirred at 120 °C for 12 h. After this time, the mixture was cooled to room temperature and the product was precipitated with hot acetone and collected by filtration. The green solid product was washed successively with hot ethyl acetate, $CHCl_3$, *n*-hexane, CCl_4 and diethylether. The resulting hygroscopic product was dried over phosphorous pentoxide. MP > 240 °C, Yield: 0.16 g (86%). UV/Vis (DMSO): λ_{max} nm (log ε) 337 (4.60), 631 (4.30), 701 (5.02). IR [(KBr) ν_{max}/cm^{-1}]: 3046 (Ar-CH), 2953 (CH), 1614 (C=N), 1564 (C=C), 1491, 1245 (S=O), 1105 (S=O), ^1H NMR (DMSO-d_6): δ, ppm 8.58–8.10 (m, 28H, Pc-H and Pyridyl-H), 4.91 (m, 12H, CH_3). Calc. for $C_{56}H_{50}N_{12}O_{13}S_6GaCl$ (+5H_2O): C 48.16, H 3.61, N 12.03%; Found: C 48.83, H 3.17, N 12.77%. MS (ESI-MS) *m*/*z*: Calc. for $C_{56}H_{40}N_{12}O_8S_6GaCl$, 1306.5; Found 1079.3 $[M\text{-}Cl\text{-}2SO_4]^+$.

2.5.6. 1,(4)-Tetrakis-[(N-methyl-2-mercaptopyridine)phthalocyaninato] chloroindium(III) sulphate (***Qnp-InPc***, Scheme 2)

Synthesis and purification was as outlined for ***Qnp-GaPc*** except compound ***np-InPc*** was employed instead of compound ***np-GaPc***. The amounts of the reagents employed were: ***np-InPc*** (0.190 g, 0.177 mmol), excess DMS (0.168 mL, 1.77 mmol) in DMF (5 mL). MP > 240 °C, Yield: 0.15 g (77%). UV/Vis (DMSO): λ_{max} nm (log ε) 323 (4.60), 632 (4.29), 703 (4.95). IR [(KBr) ν_{max}/cm^{-1}]: 3055 (Ar-CH), 2948 (CH), 1614 (C=N), 1563 (C=C), 1486, 1238 (S=O), 1159 (S=O), ^1H NMR (DMSO-d_6): δ, ppm 9.32–7.86 (m, 28H, Pc-H and Pyridyl-H), 4.86 (m, 12H, CH_3). Calc. for $C_{56}H_{48}N_{12}O_{12}S_6InCl$ (+4H_2O): C 47.24, H 3.40, N 11.81%; Found: C 47.67, H 3.09, N 12.56%. MS (ESI-MS) *m*/*z*: Calc. for $C_{56}H_{40}N_{12}O_8S_6InCl$, 1351.6; Found 1123.3 $[M\text{-}Cl\text{-}2SO_4]^+$.

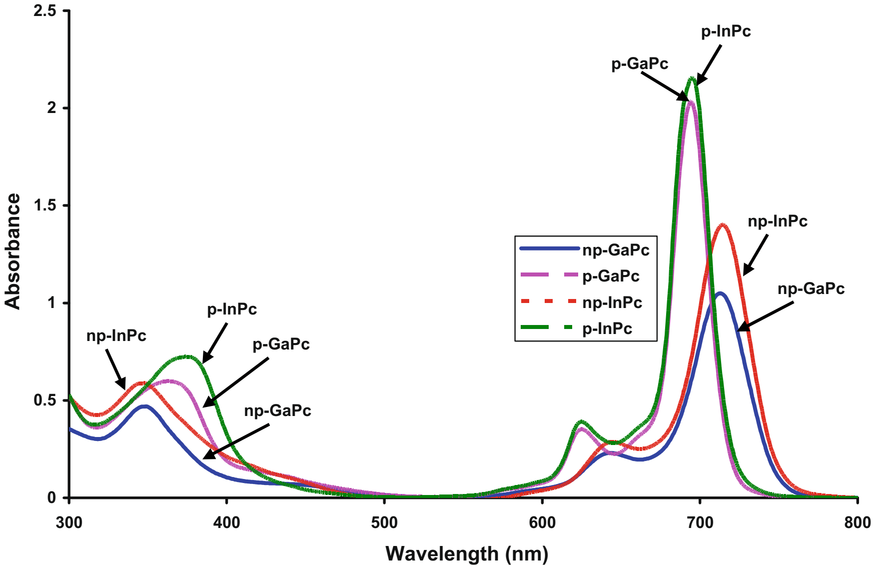

Fig. 1. Absorption spectra of tetra-substituted gallium(III) and indium(III) phthalocyanines (**np-GaPc, p-GaPc, np-InPc** and **p-InPc**) in DMSO. Concentration = 1 × 10^{-5} M.

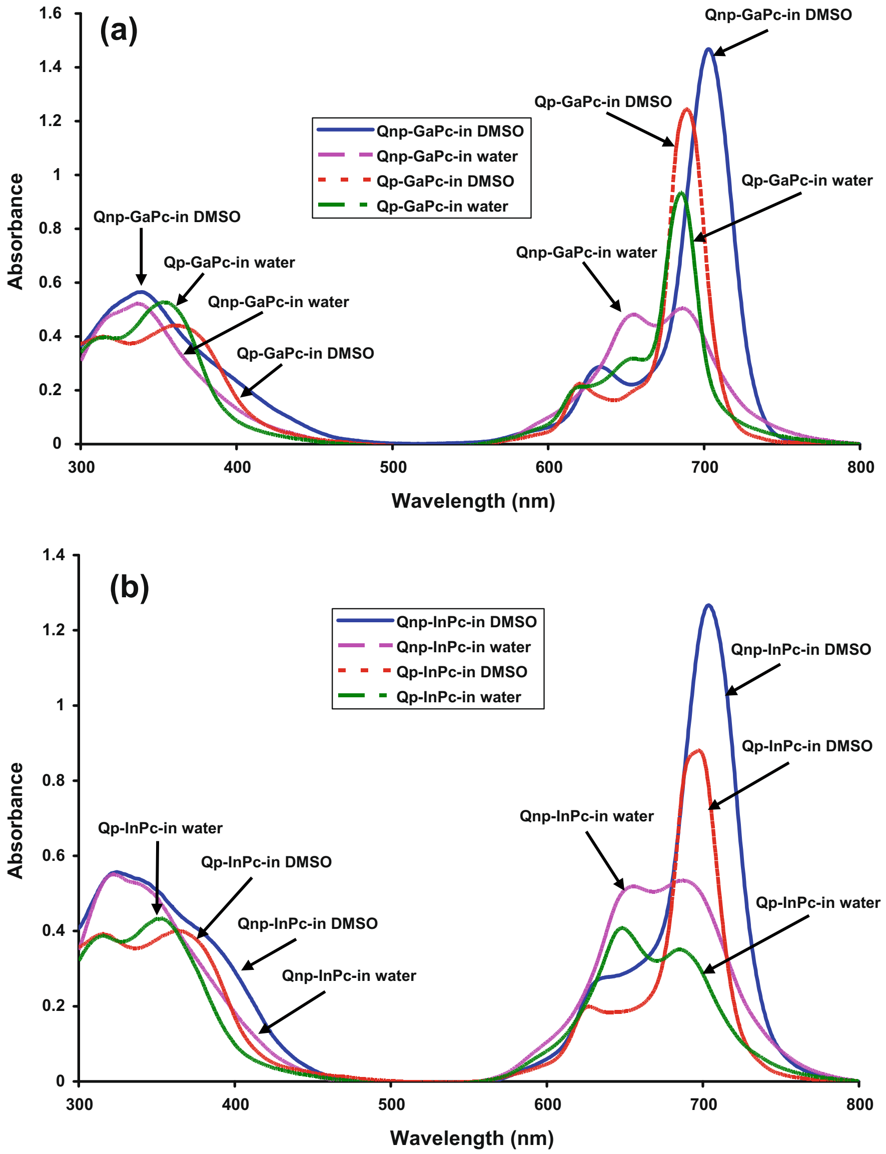

Fig. 2. Absorption spectra of: (a) tetra-substituted quaternized gallium(III) phthalocyanines (**Qnp-GaPc** and **Qp-GaPc**) and (b) tetra-substituted quaternized indium(III) phthalocyanines (**Qnp-InPc** and **Qp-InPc**) in DMSO and water. Concentration = 1 × 10^{-5} M.

2.5.7. *2,(3)-Tetrakis-[(N-methyl-2-mercaptopyridine)phthalocyaninato] chlorogallium(III) sulphate (**Qp-GaPc**, Scheme 2)*

Synthesis and purification was as outlined for ***Qnp-GaPc*** except compound ***p-GaPc*** was employed instead of compound ***np-GaPc***. The amounts of the reagents employed were: ***p-GaPc*** (0.190 g, 0.177 mmol), excess DMS (0.168 mL, 1.77 mmol) in DMF (5 mL). MP > 240 °C, Yield: 0.15 g (81%). UV/Vis (DMSO): λ_{max} nm (log ε) 360 (4.49), 619 (4.19), 689 (4.94). IR [(KBr) ν_{max}/cm^{-1}]: 3052 (Ar-CH), 2949 (CH), 1616 (C=N), 1565 (C=C), 1493, 1223 (S=O), 1094 (S=O), ^{1}H NMR (DMSO-d$_6$): δ, ppm 9.99–7.35 (m, 28H, Pc-H and Pyridyl-H), 4.53 (m, 12H, CH$_3$). Calc. for $C_{56}H_{50}N_{12}O_{13}S_6GaCl$ (+5H$_2$O): C 48.16, H 3.61, N 12.03%; Found: C 48.73, H 3.31, N 12.95%. MS (ESI-MS) *m*/*z*: Calc. for $C_{56}H_{40}N_{12}O_8S_6GaCl$, 1306.5; Found 1079.3 [M-Cl-2SO$_4$]$^+$.

2.5.8. *2,(3)-Tetrakis-[(N-methyl-2-mercaptopyridine)phthalocyaninato] chloroindium(III) sulphate (**Qp-InPc**, Scheme 2)*

Synthesis and purification was as outlined for ***Qnp-GaPc*** except compound ***p-InPc*** was employed instead of compound ***np-GaPc***. The amounts of the reagents employed were: ***p-InPc*** (0.190 g, 0.177 mmol), excess DMS (0.168 mL, 1.77 mmol) in DMF (5 mL). MP > 240 °C, Yield: 0.14 g (72%). UV/Vis (DMSO): λ_{max} nm (log ε) 361 (4.46), 625 (4.15), 692 (4.80). IR [(KBr) ν_{max}/cm^{-1}]: 3055 (Ar-CH), 2953 (CH), 1616 (C=N), 1565 (C=C), 1489, 1226 (S=O), 1111 (S=O), ^{1}H NMR (DMSO-d$_6$): δ, ppm 9.47–7.46 (m, 28H, Pc-H and Pyridyl-H), 4.57 (m, 12H, CH$_3$). Calc. for $C_{56}H_{42}N_{12}O_9S_6InCl$ (+H$_2$O): C 49.11, H 3.09, N 12.27%; Found: C 49.17, H 3.79, N 12.70%. MS (ESI-MS) *m*/*z*: Calc. for $C_{56}H_{40}N_{12}O_8S_6InCl$, 1351.6; Found 1123.3 [M-Cl-2SO$_4$]$^+$.

3. Results and discussion

3.1. *Ground state electronic absorption and fluorescence spectra*

The electronic spectra of the studied gallium(III) and indium(III) Pc complexes showed characteristic absorption in the Q band region at around 685–716 nm in DMSO, Table 1. The B-bands were observed at around 350 nm (Figs. 1 and 2). The spectra showed monomeric behaviour evidenced by a single (narrow) Q band, typical of metallated phthalocyanine complexes in DMSO [50]. In DMSO, the Q bands were observed at: 716 (**np-GaPc**), 695 (**p-GaPc**), 701 (**Qnp-GaPc**), 689 (**Qp-GaPc**), 714 (**np-InPc**), 695 (**p-InPc**), 703 (**Qnp-InPc**), and 692 (**Qp-InPc**), Table 1. The red-shifts were observed for gallium(III) and indium(III) Pc complexes following substitution. In DMSO, the quaternization caused 15 nm and 11 nm blue-shifts for non-peripheral gallium(III) and indium(III) Pc complexes, respectively. The quaternization also caused 6 nm and 3 nm blue-shifts for peripheral gallium(III) and indium(III) Pc complexes, respectively, which is smaller than non-peripheral blue-shifts. The lone pair electrons of the nitrogen atom of the substituents in non-quaternized complexes **(np-GaPc, p-GaPc, np-InPc** and **p-InPc)** are delocalized into the ring and ultimately leading to a red-shifting. However when these lone pair electrons are engaged as in quaternized complexes (**Qnp-GaPc, Qp-GaPc, Qnp-InPc** and **Qp-InPc**) and its mesomeric contribution to the ring electron density is lost.

The Q bands of the non-peripheral substituted complexes are red-shifted when compared to the corresponding peripheral substituted complexes in DMSO (Figs. 1 and 2). The red-shifts are 21 nm between **np-GaPc** and **p-GaPc**, 12 nm between **Qnp-GaPc** and **Qp-GaPc**, 19 nm between **np-InPc** and **p-InPc**, and 11 nm between **Qnp-InPc** and **Qp-InPc**. The observed red spectral shifts are typical of Pcs with substituents at the non-peripheral positions and have been explained in the literature [51,52]. The B-bands are broad due to the superimposition of the B_1 and B_2 bands in the 320 to 370 nm region. In water, the absorption spectra of quaternized complexes (**Qnp-GaPc, Qnp-InPc** and **Qp-InPc)** showed cofacial aggregation, as evidenced by the presence of two non-vibrational peaks in the Q band region, Fig. 2a and b, Table 1. The lower energy (red-shifted) bands at 686 for **Qnp-GaPc**, 685 for **Qnp-InPc** and 686 nm for **Qp-InPc** are due to the monomeric species, while the higher energy (blue-shifted) bands at 653 for **Qnp-GaPc**, 652 for **Qnp-InPc** and 649 nm for **Qp-InPc** is due to the

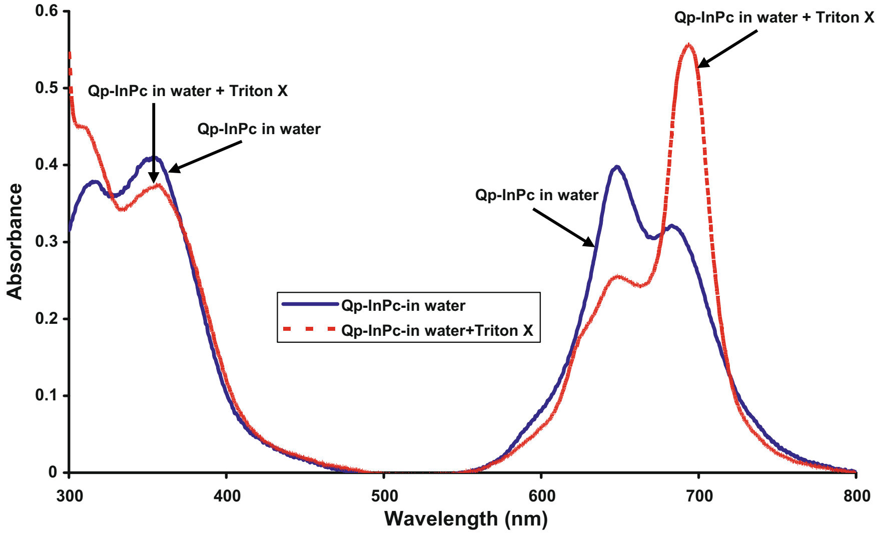

Fig. 3. Absorption spectral changes for complex **Qp-InPc** observed on addition of Triton X-100 (0.1 mL) in water. [**Qp-InPc**] = 1 × 10^{-5} M.

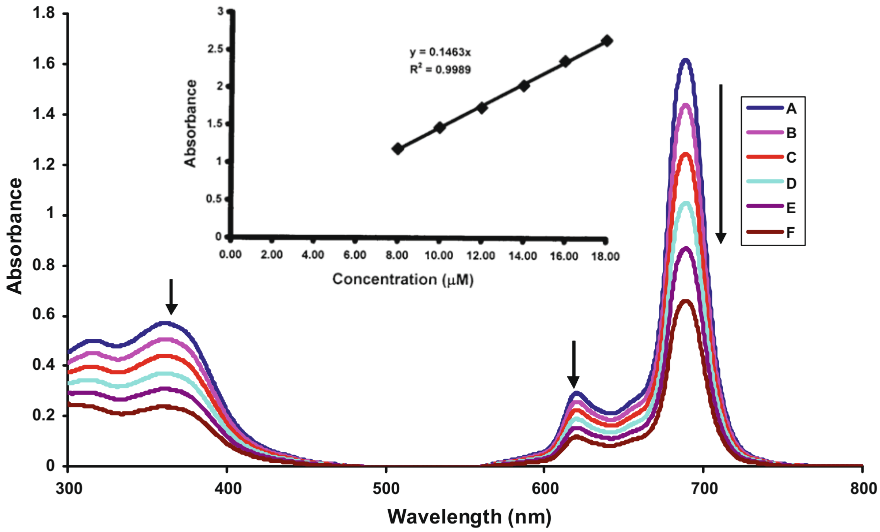

Fig. 4. Aggregation behaviour of **Qp-GaPc** in DMSO at different concentrations: 18 × 10^{-6} (A), 16 × 10^{-6} (B), 14 × 10^{-6} (C), 12 × 10^{-6} (D), 10 × 10^{-6} (E), 8 × 10^{-6} (F) M. (Inset: Plot of absorbance versus concentration).

aggregated species. Surprisingly, the **Qp-GaPc** did not show aggregation in water (Fig. 2a). The Q band of **Qp-InPc** in DMSO is distorted (Fig. 2b). We suggest that **Qp-InPc** complex is more aggregated than **Qnp-InPc** in DMSO. Aggregation is generally decreasing the intensity of the Pc molecules.

Addition of Triton X-100 (0.1 mL) to an aqueous solution of quaternized indium(III) Pc complexes (**Qnp-InPc** and **Qp-InPc**) (Concentration = 1.0×10^{-5}) brought about considerable increase in intensity of the low energy side of the Q band (Fig. 3), suggesting that the molecules are aggregated and that addition of Triton X-100 breaks up the aggregates. But spectrum of non-peripheral substituted quaternized gallium(III) Pc complex (**Qnp-GaPc**) did not show any change with the addition of Triton X-100 to an aqueous solution of this complex. This suggests that Triton X-100 molecules could be penetrate among the indium(III) Pc complexes due to the larger indium metal.

In this study, the aggregation behaviour of the gallium(III) and indium(III) Pc complexes (**np-GaPc, np-InPc, p-GaPc, p-InPc, Qnp-GaPc, Qnp-InPc, Qp-GaPc** and **Qp-InPc**) were investigated at different concentrations in DMSO (Fig. 4, for complex **Qp-GaPc** as an example). The studied gallium(III) and indium(III) Pc complexes did not show aggregation in DMSO.

Fig. 5 shows fluorescence emission, absorption and excitation spectra of complexes **p-GaPc** and **np-InPc** in DMSO and **Qnp-GaPc** in aqueous solution as examples of the studied gallium(III) and indium(III) Pc complexes. Fluorescence emission peaks were listed in Table 1. The observed Stokes shifts were within the region observed for gallium(III) and indium(III) Pc complexes. All gallium(III) Pc complexes (**np-GaPc, p-GaPc, Qnp-GaPc** and **Qp-GaPc**) showed similar fluorescence behaviour in DMSO (Fig. 5a for complex **p-GaPc** as an example). The excitation spectra were similar to absorption spectra and both were mirror images of the fluorescent spectra for all gallium(III) Pc complexes in DMSO. The proximity of the wavelength of each component of the Q band absorption to the Q band maxima of the excitation spectra for all gallium(III) Pc complexes suggest that the nuclear configurations of the ground and excited states are similar and not affected by excitation. For studied indium(III) Pc complexes (**np-InPc, p-InPc, Qnp-InPc**

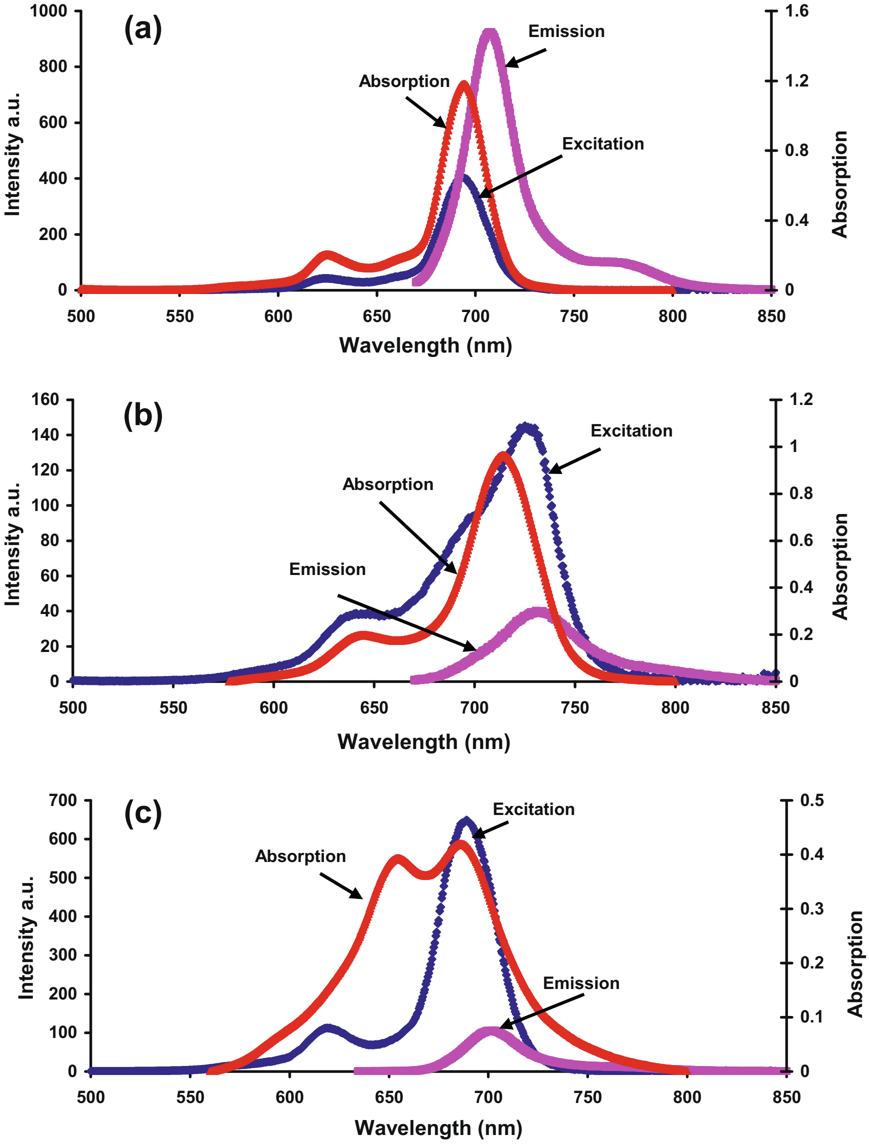

Fig. 5. Absorption, excitation and emission spectra of: (a) **p-GaPc** in DMSO, (b) **np-InPc** in DMSO and (c) **Qnp-GaPc** in water. Excitation wavelengths: 660 nm for **p-GaPc** and **np-InPc** and 625 nm for **Qnp-GaPc**.

and **Qp-InPc**), the shapes of excitation spectra were different from the absorption spectra in that the Q band of the excitation showed splitting unlike the narrow Q band of the absorption in DMSO (Fig. 5b for complex **np-InPc** as an example). This suggests that there are changes in the molecule following excitation most likely due to loss of symmetry, or change in aggregation status following excitation. Thus the Q band maxima of the excitation and absorption spectra were different (Table 1) due to the differences in the ground and excited state species. The difference in the behaviour of indium(III) Pc complexes on excitation could be due to the larger indium metal being more displaced from the core of the Pc ring, and the displacement being more pronounced on excitation hence a loss of symmetry. In aqueous media for the water-soluble quaternized gallium(III) and indium(III) Pc complexes (**Qnp-GaPc, Qp-GaPc** and **Qp-InPc**), the excitation spectra were different from absorption spectra in that one Q band is observed instead of the split Q band observed in absorption (Fig. 5c for complex **Qnp-GaPc** as an example). This observation is typical of aggregated species. Aggregated MPc complexes are not known [53] to fluoresce since aggregation lowers the photoactivity of molecules through dissipation of energy by aggregates. The quaternized non-peripheral substituted indium phthalocyanine complex (**Qnp-InPc**) showed very low fluorescence in aqueous media.

3.2. Fluorescence lifetimes and quantum yields

The fluorescence quantum yields (Φ_F) for non-ionic gallium(III) and indium(III) Pc complexes (**np-GaPc, np-InPc, p-GaPc** and **p-InPc**) in DMSO and for quaternized ionic complexes (**Qnp-GaPc, Qnp-InPc, Qp-GaPc** and **Qp-InPc**) in both DMSO and water are given in Table 2. The Φ_F values of all studied gallium(III) and indium(III) Pc complexes are typical of gallium(III) and indium(III) Pc complexes [54,55]. The quaternized ionic Pc complexes showed aggregation in water. The Φ_F values of these complexes are for the mixture of the monomer-aggregated Pc species in the water. The Φ_F values of the substituted gallium(III) Pc complexes are lower compared to unsubstituted gallium(III) Pc complex in DMSO, which implies that the presence of the 2-mercaptopyridine substituents certainly results in fluorescence quenching. For indium(III) Pc complexes, the Φ_F value of the peripheral substituted indium(III) Pc complex is higher than unsubstituted indium(III) Pc complex while the non-peripheral substituted indium(III) Pc complex is lower than unsubstituted indium(III) Pc complex which suggesting more quenching by peripheral substitution compared to non-peripheral substitution. The Φ_F values of gallium(III) Pc complexes (in both of DMSO and water) were higher than indium(III) Pc complexes because of the indium is very heavy metal, Table 2. The peripheral substituted complexes show marginally higher Φ_F values in both of DMSO and water, compared to non-peripheral substituted derivatives, suggesting not as much of quenching of the excited singlet state by peripheral substitution compared to the non-peripheral substitution. The non-ionic phthalocyanine complexes (**np-GaPc, np-InPc, p-GaPc, p-InPc**) show larger Φ_F values compared to the corresponding quaternarized ionic Pc complexes (**Qnp-GaPc, Qnp-InPc, Qp-GaPc** and **Qp-InPc**) in DMSO. Comparing DMSO and water, the quaternarized ionic Pc complexes (**Qnp-GaPc, Qnp-InPc, Qp-GaPc** and **Qp-InPc**) show larger Φ_F values in DMSO than in water. This is attributed to the higher viscosity of DMSO than that of water. As expected on grounds of the higher viscosity of DMSO compared to that of water, Φ_F values of the quaternarized ionic complexes (**Qnp-GaPc, Qnp-InPc, Qp-GaPc** and **Qp-InPc**) are higher in DMSO than in water. The relationship between Φ_F and the viscosity (η) of the solvent has been derived, and is given by the Forster–Hoffmann [56]:

$$\log\Phi_F = C + x\log\eta \quad (8)$$

where C is a temperature-dependent constant and x, a fluorophore dependent constant.

Table 2
Photophysical and photochemical parameters of unsubstituted, non-peripheral and peripheral tetra-substituted gallium(III) and indium(III) phthalocyanine complexes in DMSO and water.

Compound	Solvent	Φ_F	τ_F (ns)	τ_0 (ns)	[a]$k_F/10^8$ (s^{-1})	$\Phi_d/10^{-4}$	Φ_Δ
GaPc[b]	DMSO	0.30	3.71	11.96	0.83	0.09	0.41
np-GaPc	DMSO	0.20	3.41	14.22	0.70	0.27	0.67
p-GaPc	DMSO	0.22	3.50	9.71	1.03	14.44	0.76
Qnp-GaPc	DMSO	0.11	0.78	9.72	1.03	41.91	0.52
	H_2O	0.021	0.38	16.99	0.58	0.41	0.29
Qp-GaPc	DMSO	0.12	1.57	13.10	0.76	38.61	0.75
	H_2O	0.074	1.41	19.06	0.52	0.10	0.26
InPc[b]	DMSO	0.018	0.90	50.20	0.19	0.34	0.67
np-InPc	DMSO	0.017	0.17	9.94	1.00	0.36	0.75
p-InPc	DMSO	0.029	0.26	9.18	1.09	21.23	0.85
Qnp-InPc	DMSO	0.0028	0.024	8.84	1.13	0.68	0.57
	H_2O	–	–	–	–	3.73	0.80
Qp-InPc	DMSO	0.021	0.36	17.27	0.58	22.42	0.79
	H_2O	0.0008	<0.1	38.00	0.26	1.29	0.40

[a] k_F is the rate constant for fluorescence. Values calculated using $k_F = \Phi_F/\tau_F$.

[b] Data from [55].

Fluorescence lifetime (τ_F) refers to the average time a molecule stays in its excited state before fluorescing, and its value is directly related to that of Φ_F; i.e. the longer the lifetime, the higher the quantum yield of fluorescence. Any factor that shortens the fluorescence lifetime of a fluorophore indirectly reduces the value of Φ_F. Such factors include internal conversion and intersystem crossing. As a result, the nature and the environment of a fluorophore determine its fluorescence lifetime.

τ_F values (Table 2) were calculated using the Strickler–Berg equation. The τ_F values of the substituted gallium(III) and indium(III) Pc complexes are lower compared to unsubstituted gallium(III) and indium(III) Pc complexes in DMSO, suggesting more quenching by substitution. τ_F values are lower for non-peripheral complexes (**np-GaPc, np-InPc, Qnp-GaPc** and **Qnp-InPc**) when compared to peripheral complexes (**p-GaPc, p-InPc, Qp-GaPc** and **Qp-InPc**), Table 2, suggesting more quenching by peripheral substitution compared to non-peripheral substitution. However the τ_F values are typical for gallium(III) and indium(III) Pc complexes [53,54]. The τ_F values of gallium(III) Pc complexes (in both of DMSO and water) were higher than indium(III) Pc complexes because of the indium is very heavy metal, Table 2.

The natural radiative lifetime (τ_0) and the rate constants for fluorescence (k_F) values are also given in Table 2. But there was no clear trend found for τ_0 and k_F values among the studied gallium(III) and indium(III) Pc complexes.

3.3. Singlet oxygen quantum yields

Energy transfer between the triplet state of photosensitizers and ground state molecular oxygen leads to the production of singlet oxygen. There is a necessity of high efficiency of transfer of energy between excited triplet state of MPc and ground state of oxygen to generate large amounts of singlet oxygen, essential for PDT.

The singlet oxygen quantum yields (Φ_Δ), give an indication of the potential of the complexes as photosensitizers in applications where singlet oxygen is required, (e.g. for Type II mechanism). The Φ_Δ values were determined using a chemical method (DPBF in DMSO and ADMA in water). The disappearance of DPBF or ADMA was monitored using UV–vis spectrophotometer (Fig. 6a using DPBF for complex **p-GaPc** in DMSO and Fig. 6b using ADMA for complex **Qnp-InPc** in water). Many factors are responsible for the magnitude of the determined quantum yield of singlet oxygen

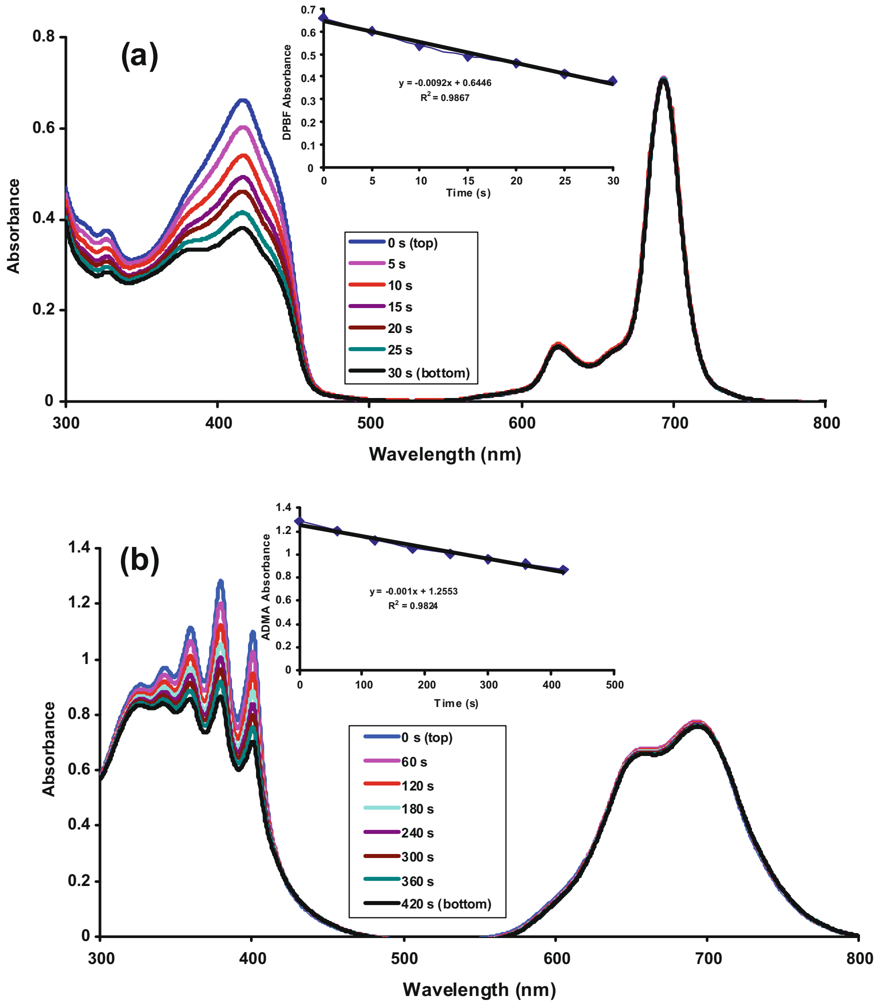

Fig. 6. A typical spectrum for the determination of singlet oxygen quantum yield of: (a) **p-GaPc** in DMSO using DPBF as a singlet oxygen quencher and (b) **Qnp-InPc** in water using ADMA as a singlet oxygen quencher. Concentration = 1 × 10^{-5} M. (Inset: plots of DPBF or ADMA absorbance versus time.)

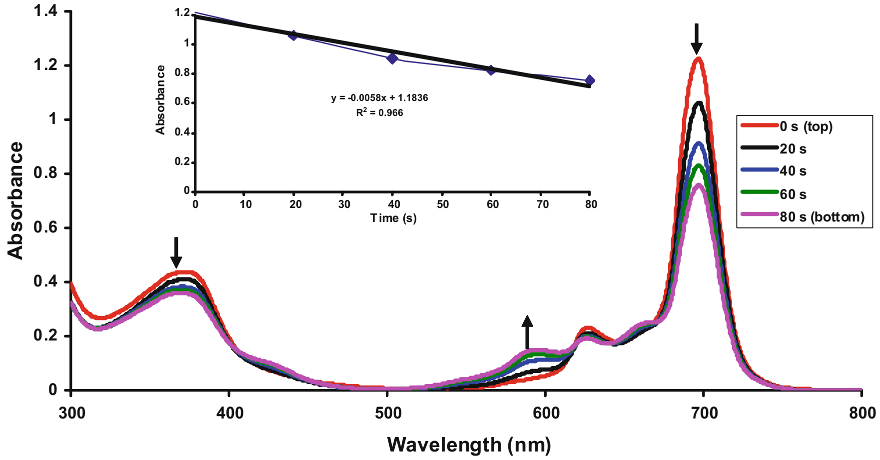

Fig. 7. The photodegradation of **p-InPc** in DMSO showing the disappearance of the Q band and appearance of the reduction band at 20 s intervals. (Inset: plot of Q band absorbance versus time.)

including; triplet excited state energy, ability of substituents and solvents to quench the singlet oxygen, the triplet excited state lifetime and the efficiency of the energy transfer between the triplet excited state and the ground state of oxygen. There was no decrease in the Q band of formation of new bands during Φ_Δ determinations (Fig. 6).

Table 2 shows that the values of Φ_Δ are higher for substituted gallium(III) and indium(III) Pc complexes (**np-GaPc, np-InPc,**

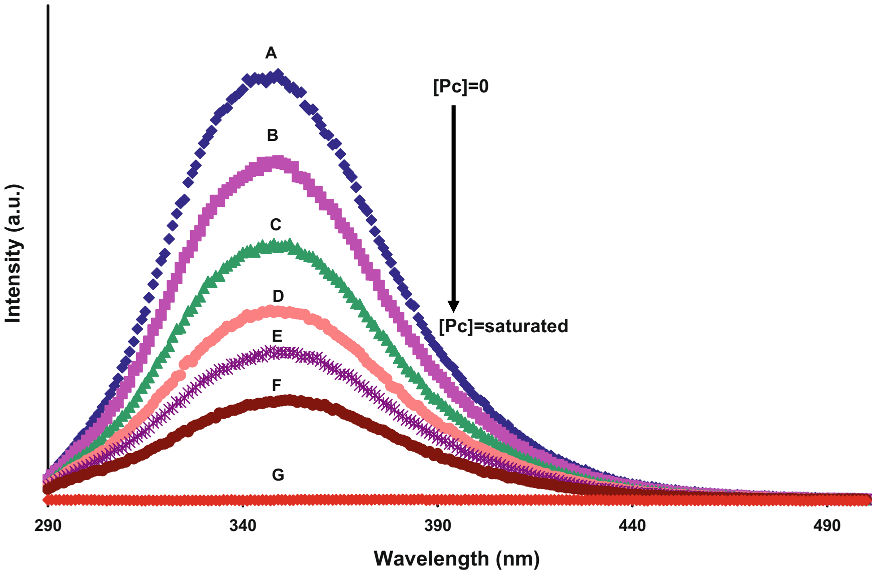

Fig. 8. Fluorescence emission spectral changes of BSA ($C = 3.00 \times 10^{-5}$ M) on addition of varying concentrations of **Qnp-InPc** in water. [**Qnp-InPc**]: $A = 0$, $B = 1.66 \times 10^{-6}$, $C = 3.33 \times 10^{-6}$, $D = 5.00 \times 10^{-6}$, $E = 6.66 \times 10^{-6}$, $F = 8.33 \times 10^{-6}$ M, G = saturated with **Qnp-InPc** .

p-GaPc, p-InPc, Qnp-GaPc, Qp-GaPc and **Qp-InPc**) when compared to respective unsubstituted gallium(III) and indium(III) Pc except for complex **Qnp-InPc** which is lower than unsubstituted **InPc** due to a little aggregation in DMSO. The peripheral substituted complexes (**p-GaPc, Qp-GaPc, p-InPc**, and **Qp-InPc**) are higher Φ_Δ values when compared to the non-peripheral complexes (**np-GaPc**, **Qnp-GaPc**, **np-InPc**, and **Qnp-InPc**) in DMSO. On the contrary in water, the non-peripheral substituted complexes (**np-GaPc**, **Qnp-GaPc**, **np-InPc**, and **Qnp-InPc**) are higher Φ_Δ values when compared to the peripheral complexes (**p-GaPc**, **Qp-GaPc**, **p-InPc**, and **Qp-InPc**).

Table 2 shows that lower Φ_Δ values are observed in aqueous solutions compared to in DMSO. The low Φ_Δ in water compared to other solvents such as deuterated water and DMSO was explained [57] by the fact that singlet oxygen absorbs at 1270 nm, and water, which absorbs around this wavelength has a great effect on singlet oxygen lifetime, while DMSO which exhibits little absorption in this region has longer singlet oxygen lifetimes than water, resulting in large Φ_Δ values in DMSO. However the value of Φ_Δ for **Qnp-InPc** is higher in water (0.80) than in DMSO (0.57).

Quaternarized ionic gallium(III) and indium(III) Pc complexes (**Qnp-GaPc**, **Qp-GaPc**, **Qnp-InPc**, and **Qp-InPc**) showed lower Φ_Δ values when compared to corresponding non-ionic complexes (**np-GaPc**, **p-GaPc**, **np-InPc**, and **p-InPc**) in DMSO.

The Φ_Δ values of indium(III) Pc complexes (in both of DMSO and water) are higher than gallium(III) Pc complexes because of the indium is very heavy metal. The populations of the molecules on the triplet state are higher for indium(III) Pc complexes than gallium(III) Pc complexes.

3.4. Photodegradation studies

Degradation of the molecules under irradiation can be used to study their stability and this is especially important for those

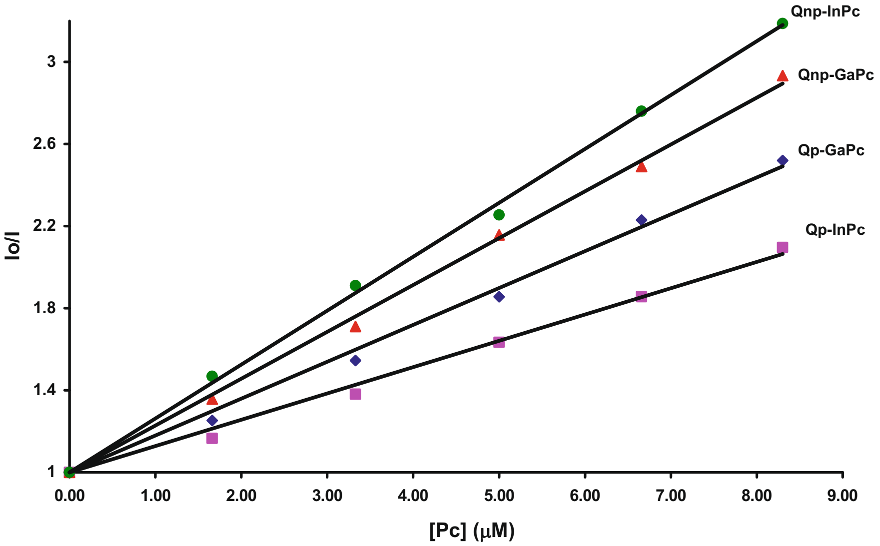

Fig. 9. Stern–Volmer plots of tetra substituted gallium(III) and indium(III) phthalocyanines quenching of BSA in water. [BSA] = 3.00×10^{-5} M in water. [Pc] = 0, 1.66×10^{-6}, 3.33×10^{-6}, 5.00×10^{-6}, 6.66×10^{-6}, 8.33×10^{-6} M.

molecules intended for use in photocatalysis. The collapse of the absorption spectra without any distortion of the shape confirms clean photodegradation not associated with phototransformation into different forms of MPc absorbing in the visible region.

Fig. 7 shows that for gallium(III) and indium(III) Pc complexes, there was a change in spectra following photodegradation. The spectral changes involved a decrease in the Q band and an increase in the absorption near 590 nm, suggesting that this band is due to reduction products of the complexes. These spectral changes were only observed in DMSO. The first ring reduction in MPc complexes is characterized by a decrease in the Q band and the formation of weak bands between 500 and 600 nm [58]. When the degradated solutions of the gallium(III) and indium(III) Pc complexes were oxidized with bromine as oxidation agent the intensity of the Q band was increased and the reduction band at around 600 nm was disappeared. Thus, we propose that during photodegradation, the gallium(III) and indium(III) Pc complexes were partly transformed to an anion (Pc^{-3}) species. This type of transformation has been observed before during the photodegradation of gallium(III) and indium(III) Pc complexes [54]. The suggested mechanism for the formation of Pc^{-3} in the presence of H donors is shown by Eqs. (9)–(11):

$$\mathrm{MPc} + h\nu \rightarrow {}^{3}\mathrm{MPc}^{*} \tag{9}$$

$$^{3}\mathrm{MPc}^{*} + \mathrm{S-H} \rightarrow \mathrm{MPc}^{\cdot-} + \mathrm{S-H}^{\cdot+} \tag{10}$$

$$\mathrm{MPc}^{\cdot-} + \mathrm{O_2} \rightarrow \mathrm{MPc} + \mathrm{O_2^{\cdot-}} \tag{11}$$

S = solvent

All the studied gallium(III) and indium(III) Pc complexes showed about the same stability with Φ_d of the order of between 10^{-3} and 10^{-4}. The Φ_d values, found in this study, are similar gallium(III) and indium(III) Pc complexes having different substituents on the phthalocyanine ring in literature [20–22,54,55]. Stable zinc phthalocyanine complexes show Φ_d values as low as 10^{-6} and for unstable molecules, values of the order of 10^{-3} have been reported [53]. It seems studied gallium(III) and indium(III) Pc complexes show also similar Φ_d values and stability with zinc Pc complexes.

Table 3
Binding and fluorescence quenching data for interaction of BSA with quaternized gallium(III) and indium(III) phthalocyanine complexes in water.

Compound	$K_{SV}^{BSA}/10^5$ (M^{-1})	$k_q/10^{13}$ (M^{-1} s^{-1})	$K_b/10^{-6}$ (M^{-1})	n
Qnp-GaPc	2.28	2.28	4.78	1.26
Qp-GaPc	1.79	1.79	5.49	1.33
Qnp-InPc	2.62	2.62	4.22	1.24
Qp-InPc	1.28	1.28	7.41	1.23

3.5. Interaction of quaternized ionic gallium(III) and indium(III) phthalocyanine complexes with BSA

Fig. 8 shows the fluorescence emission spectra of BSA in the presence of different concentrations of **Qnp-InPc** in water as an example. The quaternized gallium(III) and indium(III) Pc complexes are mixtures of aggregated and unaggregated species. The total concentrations of the complexes are mixture of the monomer and aggregated species. We calculated the percentage aggregation (% Agg) of these complexes using the equation described in the literature [59,60]. The aggregation percentages are 6% for **Qnp-GaPc**, 10% for **Qnp-InPc**, 50% for **Qp-GaPc** and 42% for **Qp-InPc**. The non-peripheral substituted Pc complexes having lower % Agg values which may be due to reduced aggregation tendencies when the substitution is at the non-peripheral position of the Pc skeleton [61]. The BSA fluorescence at 348 nm is mainly attributable to tryptophan residues in the macromolecule. BSA and the respective quaternized ionic Pc complexes exhibit reciprocated fluorescence quenching on one another; hence it was possible to determine Stern–Volmer quenching constants (K_{SV}). The slope of the plots shown at Fig. 9 gave K_{SV} values and listed in Table 3, suggest that BSA fluorescence quenching is more effective for quaternized non-peripheral substituted Pc complexes (**Qnp-GaPc** and **Qnp-InPc**) than quaternized peripheral substituted Pc complexes (**Qp-GaPc** and **Qp-InPc**) in water. Using the approximate fluorescence lifetime of BSA (10 ns) [48,49], the bimolecular quenching constant (k_q) was determined (Eq. (7)). These values are of the order of 10^{13} M^{-1} s^{-1}, which exceed the proposed value of 10^{10} M^{-1} s^{-1} for diffusion-controlled (dynamic) quenching (according to the Einstein–Smoluchowski approximation) at room temperature [62]. This also, is an indication that the mechanism of BSA quenching by quaternized Pc complexes (**Qnp-GaPc**, **Qp-GaPc**, **Qnp-InPc**

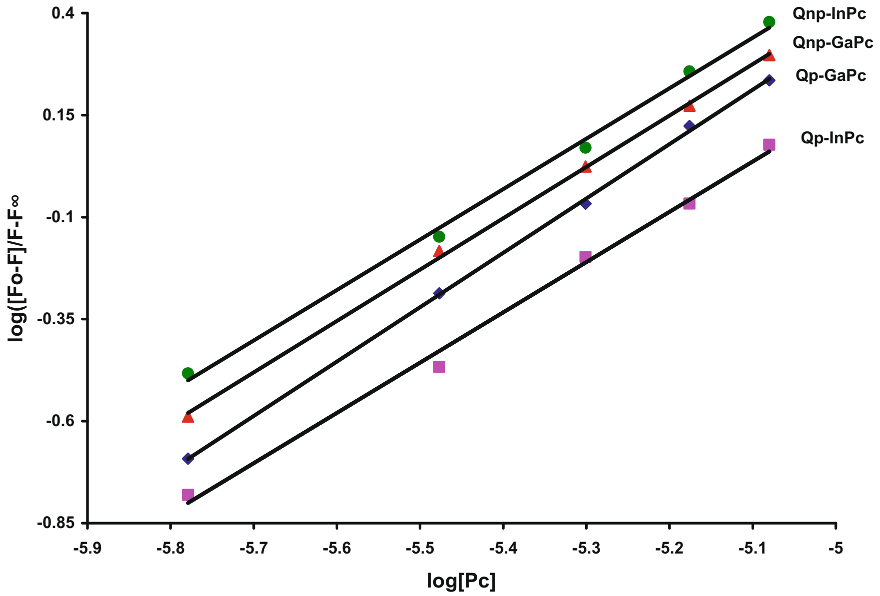

Fig. 10. Determination of tetra substituted gallium(III) and indium(III) phthalocyanine-BSA binding constant (and number of binding sites on BSA). [BSA] = 3.00×10^{-5} M and [Pc] = 0, 1.66×10^{-6}, 3.33×10^{-6}, 5.00×10^{-6}, 6.66×10^{-6}, 8.33×10^{-6} M in water.

and **Qp-InPc**) is not diffusion-controlled (i.e., not dynamic quenching, but static quenching). The k_q values are larger for quaternized non-peripheral substituted Pc complexes (**Qnp-GaPc** and **Qnp-InPc**) than quaternized peripheral substituted Pc complexes (**Qp-GaPc** and **Qp-InPc**) in water. The binding constants (K_b) and number of binding sites (n) on BSA were obtained using Eq. (5) and the results are shown in Table 3. The slope of the plots shown at Fig. 10 gave n values and the intercepts of these plots gave K_b values. The values of K_b and n are typical of MPc-BSA interactions in aqueous solutions [45,63]. The higher K_b value for quaternized peripheral substituted Pc complexes (**Qp-GaPc** and **Qp-InPc**) implies that a peripheral substituted Pc complexes binds more strongly to BSA than the quaternized non-peripheral substituted Pc complexes (**Qnp-GaPc** and **Qnp-InPc**), probably due to steric effect at the non-peripheral position. n values of near unity suggest that both non-peripheral and peripheral substituted Pc complexes form 1:1 adducts with BSA. The decrease in the intrinsic fluorescence intensity of tryptophan with quaternized Pc concentration indicates that these complexes readily bind to BSA, which implies that the Pc molecules reach subdomains where tryptophan residues are located in BSA. This also suggests that the primary binding sites of these molecules are very close to tryptophan residues, since the occurrence of quenching requires molecular contact.

4. Conclusion

In conclusion, this work has described the synthesis, spectral, photophysical and photochemical properties of new non-peripheral and peripheral tetra-2-mercaptopyridine substituted non-ionic and quaternized ionic gallium(III) and indium(III) Pc complexes. The effect of quaternization on these properties is also presented. Solvent effect (DMSO or water) on the photophysical and photochemical properties of the quaternized derivative is investigated. Although, the photophysical and photochemical properties relevant for photosensitization gave more attractive values in DMSO, the values in water are still good enough for PDT applications. This work will certainly enrich the hitherto scanty literature on the potentials of cationic phthalocyanines as photosensitizers in PDT. All studied gallium(III) Pc complexes (**np-GaPc, p-GaPc, Qnp-GaPc** and **Qp-GaPc**) showed similar fluorescence behaviour with MPcs. The difference in the behaviours of indium(III) Pc complexes on excitation could be due to the larger indium metal being more displaced from the core of the Pc ring. The Φ_F values of the indium Pc complexes are very low due to presence of a heavier indium atom in these complexes. All studied gallium(III) and indium(III) Pc complexes have good Φ_Δ values. In particular, quaternarized non-peripheral indium(III) Pc complex (**Qnp-InPc**) has high Φ_Δ value (0.80) in water (Photosens®, which has been in use for PDT has Φ_Δ of 0.42). Thus, these complexes show potential as Type II photosensitizers for photodynamic therapy of cancer. Photoreduction of the gallium(III) and indium(III) Pc complexes was observed during photodegradation in DMSO. This study reveals that the water-soluble complexes bind strongly to serum albumin; hence they can easily be transported in the blood.

Acknowledgement

This work was supported by Gebze Institute of Technology (Project number: BAP-2007-A-01).

References

[1] C.C. Leznoff, A.B.P. Lever (Eds.), Phthalocyanines: Properties and Applications, vols. 1–4, VCH Publishers, New York, 1989–1996.
[2] N.B. McKeown, Phthalocyanine Materials, Cambridge University Press, Cambridge, 1998.
[3] K. Kadish, K.M. Smith, R. Guilard (Eds.), The Porphyrin Handbook, vols. 15–20, Academic Press, Boston, 2003.
[4] P. Gregory, J. Porphyr. Phthalocya. 4 (2000) 432–437.
[5] K. Daimon, K. Nukada, Y. Sakaguchi, R. Igarashi, J. Imag. Sci. Technol. 40 (1996) 249–253.
[6] A. Tracz, T. Makowski, S. Masirek, W. Pisula, Y.H. Geerts, Nanotechnology 18 (2007) 485303–485307.
[7] S.A. Priola, A. Raines, W.S. Caughey, Science 287 (2000) 1503–1506.
[8] E. Ben-Hur, W.S. Chan, in: K. Kadish, K.M. Smith, R. Guilard (Eds.), The Porphyrin Handbook, vol. 19, Academic Press, Boston, 2003, pp. 1–35.
[9] E. Ben-Hur, M. Green, A. Prager, R. Kol, I. Rosenthal, Photochem. Photobiol. 46 (1987) 651–656.
[10] I.J. MacDonald, T.J. Dougherty, J. Porphyr. Phthalocya. 5 (2001) 105–129.
[11] H. Ali, J.E. van Lier, Chem. Rev. 99 (1999) 2379–2450.
[12] D. Phillips, Pure Appl. Chem. 67 (1995) 117–126.
[13] R. Bonnett, Chem. Soc. Rev. 24 (1995) 19–33.
[14] A.C. Tedesco, J.C.G. Rotta, C.N. Lunardi, Curr. Org. Chem. 7 (2003) 187–196.
[15] S. Wang, Q. Gan, Y. Zhang, S. Li, H. Xu, G. Yang, ChemPhysChem 7 (2006) 935–941.
[16] Y. Chen, Y. Araki, D. Dini, Y. Liu, O. Ito, M. Fujitsuka, Mater. Chem. Phys. 98 (2006) 212–216.
[17] Y. Chen, D. Dini, M. Hanack, M. Fujitsua, O. Ito, Chem. Commun. (2004) 340–341.
[18] Y. Chen, Y. Araki, M. Fujitsuka, M. Hanack, O. Ito, S.M. O'Flaherty, W.J. Blau, Solid State Commun. 131 (2004) 773–778.
[19] V. Chauke, T. Nyokong, J. Mol. Catal. A: Chem. 289 (2008) 9–13.
[20] A. Ogunsipe, M. Durmuş, T. Nyokong, J. Porphyr. Phthalocya. 11 (2007) 635–644.
[21] M. Durmuş, T. Nyokong, Inorg. Chem. Commun. 10 (2007) 332–338.
[22] M. Durmuş, T. Nyokong, Photochem. Photobiol. Sci. 6 (2007) 659–668.
[23] P. Zimcik, M. Miletin, Z. Musil, K. Kopecky, L. Kubza, D. Brault, J. Photochem. Photobiol. A: Chem. 183 (2006) 59–69.
[24] M.P. de Filippis, D. Dei, L. Fantetti, G. Roncucci, Tetrahedron Lett. 41 (2000) 9143–9147.
[25] I. Scalise, E.N. Durantini, Bioorg. Med. Chem. 13 (2005) 3037–3045.
[26] S.R. Wood, J.A. Holroyd, S.B. Brown, Photochem. Photobiol. 65 (1997) 397–402.
[27] A.P. Castano, T.N. Demidova, M.R. Hamblin, Photodiagn. Photodynam. Ther. 1 (2004) 279–293.
[28] A.G. Gürek, M. Durmuş, V. Ahsen, New J. Chem. 28 (2004) 693–699.
[29] D. Atilla, M. Durmuş, A.G. Gürek, V. Ahsen, T. Nyokong, Dalton Trans. (2007) 1235–1243.
[30] D.C. Carter, J.X. Ho, Adv. Protein Chem. 45 (1994) 153–203.
[31] T. Peters, Adv. Protein Chem. 37 (1985) 161–245.
[32] D.D. Perrin, W.L.F. Armarego, Purification of Laboratory Chemicals, second ed., Pegamon Press, Oxford, 1989.
[33] R.D. George, A.W. Snow, J. Heterocyclic Chem. 32 (1995) 495–498.
[34] J.G. Young, W. Onyebuagu, J. Org. Chem. 55 (1990) 2155–2159.
[35] N. Sehlotho, M. Durmuş, V. Ahsen, T. Nyokong, Inorg. Chem. Commun. 11 (2008) 479–483.
[36] S. Fery-Forgues, D. Lavabre, J. Chem. Ed. 76 (1999) 1260–1264.
[37] D. Maree, T. Nyokong, K. Suhling, D. Phillips, J. Porphyr. Phthalocya. 6 (2002) 373–376.
[38] P. Jacques, A.M. Braun, Helv. Chim. Acta 64 (1981) 1800–1806.
[39] H. Du, R.A. Fuh, J. Li, A. Corkan, J.S. Lindsey, Photochem. Photobiol. 68 (1998) 141–142.
[40] J.H. Brannon, D. Madge, J. Am. Chem. Soc. 102 (1980) 62–65.
[41] A. Ogunsipe, T. Nyokong, J. Photochem. Photobiol. A: Chem. 173 (2005) 211–220.
[42] N. Kuznetsova, N. Gretsova, E. Kalmkova, E. Makarova, S. Dashkevich, V. Negrimovskii, O. Kaliya, E. Luk'yanets, Russ. J. Gen. Chem. 70 (2000) 133–140.
[43] W. Spiller, H. Kliesch, D. Wöhrle, S. Hackbarth, B. Roder, G. Schnurpfeil, J. Porphyr. Phthalocya. 2 (1998) 145–158.
[44] D.M. Chipman, V. Grisaro, N. Shanon, J. Biol. Chem. 242 (1967) 4388–4394.
[45] S.M.T. Nunes, F.S. Sguilla, A.C. Tedesco, Braz. J. Med. Biol. Res. 37 (2004) 273–284.
[46] S. Lehrer, G.D. Fashman, Biochem. Biophys. Res. Commun. 23 (1966) 133–138.
[47] J.R. Lakowicz, G. Weber, Biochemistry 12 (1973) 4161–4170.
[48] C.Q. Jiang, M.X. Gao, J.X. He, Anal. Chim. Acta 452 (2002) 185–189.
[49] M. Gou, J.W. Zou, P.G. Yi, Z.C. Shang, G.X. Hu, Q.S. Yu, Anal. Sci. 20 (2004) 465–470.
[50] M.J. Stillman, T. Nyokong, in: C.C. Leznoff, A.B.P. Lever (Eds.), Phthalocyanines: Properties and Applications, vol. 1, VCH Publishers, New York, 1989 (Chapter 3).
[51] A.B. Anderson, T.L. Gorden, M.E. Kenney, J. Am. Chem. Soc. 107 (1985) 192–195.
[52] M. Konami, M. Hatano, A. Tajiri, Chem. Phys. Lett. 166 (1990) 605–608.
[53] T. Nyokong, Coord. Chem. Rev. 251 (2007) 1707–1722.
[54] M. Durmuş, T. Nyokong, Tetrahedron 63 (2007) 1385–1394.
[55] M. Durmuş, T. Nyokong, Polyhedron 26 (2007) 3323–3325.
[56] T. Förster, G. Hoffmann, Z. Phys. Chem. 75 (1971) 63–76.
[57] A. Ogunsipe, J-Y. Chen, T. Nyokong, New J. Chem. 28 (2004) 822–827.
[58] M.J. Stillman, in: C.C. Leznoff, A.B.P. Lever (Eds.), Phthalocyanines: Properties and Applications, vol. 3, VCH Publishers, New York, 1994 (Chapter 5).
[59] M. Idowu, T. Nyokong, J. Photochem. Photobiol. A: Chem. 197 (2008) 273–280.
[60] S. Khene, A. Ogunsipe, E. Antunes, T. Nyokong, J. Porphyr. Phthalocya. 11 (2007) 109–117.
[61] R.D. George, A.W. Snow, J.S. Shirk, W.R. Barger, J. Porphyr. Phthalocya. 2 (1998) 1–7.
[62] S.L. Murov, I. Carmichael, G.L. Hug, Handbook of Photochemistry, second ed., M. Decker, New York, 1993.
[63] R. Nilsson, D.R. Kearns, J. Phys. Chem. 78 (1974) 1681–1683.